Nonlinear development of weak beam–plasma instability

L. F. Ziebell, R. Gaelzer, and Peter H. Yoon

Citation: Physics of Plasmas **8**, 3982 (2001); doi: 10.1063/1.1389863
View online: http://dx.doi.org/10.1063/1.1389863
View Table of Contents: http://scitation.aip.org/content/aip/journal/pop/8/9?ver=pdfcov
Published by the AIP Publishing

Nonlinear development of weak beam–plasma instability

L. F. Ziebell[a)]
Instituto de Física, Universidade Federal do Rio Grande do Sul (UFRGS), Caixa Postal 15051, 91501-970 Porto Alegre, RS, Brazil

R. Gaelzer[b)]
Instituto de Física e Matemática, Universidade Federal de Pelotas (UFPel), Caixa Postal 354, 96010-900 Pelotas, RS, Brazil

Peter H. Yoon[c)]
Institute for Physical Science and Technology, University of Maryland, College Park, Maryland 20742

(Received 29 March 2001; accepted 12 June 2001)

Nonlinear interactions of tenuous electron beam, background, unmagnetized plasma, and self-consistently generated Langmuir and ion-sound waves are analyzed in the framework of plasma weak turbulence kinetic theory. Full numerical solutions of the complete weak turbulence equations are obtained for the first time, which show the familiar plateau formation in the electron beam distribution and concomitant quasi-saturation of primary Langmuir waves, followed by fully nonlinear processes which include three-wave decay and induced-scattering processes. A detailed analysis reveals that the scattering off ions is an important nonlinear process which leads to prominent backscattered and long-wavelength Langmuir wave components. However, it is found that the decay process is also important, and that the nonlinear development of weak Langmuir turbulence critically depends on the initial conditions. Special attention is paid to the electron-to-ion temperature ratio, T_e/T_i, and the initial perturbation level. It is found that higher values of T_e/T_i promote the generation of backscattered Langmuir wave component, and that a higher initial wave intensity suppresses the backscattered component while significantly enhancing the long-wavelength Langmuir wave component. © *2001 American Institute of Physics.*
[DOI: 10.1063/1.1389863]

I. INTRODUCTION

The study of beam–plasma (or bump-on-tail) instability and subsequent nonlinear development is a classic problem in plasma physics. Contemporary plasma turbulence theory, which began with quasilinear theory,[1,2] has largely been developed in the context of the beam–plasma instability. Attempts were made to extend the quasilinear theory to incorporate the effects of spontaneous fluctuations[3,4] and stable oscillations.[5,6] Numerical solutions of the quasilinear equation in one- and two-dimensions can also be found in the literature (see, e.g., Ref. 7). Inspired by applications to the solar type III radio burst problem, quasilinear treatment of beam–plasma instability in a system with spatial inhomogeneity along the direction of the beam propagation were extensively investigated,[8–15] and the influence of other physical effects, such as the density fluctuations,[16,17] on the beam–plasma instability development were also discussed in the literature.

It is widely accepted that the primary saturation mechanism for the bump-on-tail instability at a relatively early quasilinear stage of the evolution is the velocity–space plateau formation in the beam distribution function. Once the system has reached the quasilinear saturation stage, nonlinear wave–wave and wave–particle interactions should take over, and the plasma should exhibit turbulent behavior. However, the detailed nonlinear beam–plasma interaction process beyond the quasilinear stage is less than completely understood. One of the main reasons is the lack of comprehensive analysis of theoretical equations to interpret particle or Vlasov simulation results. Within the context of incoherent turbulent processes, the weak turbulence theory,[18–31] which generalizes the quasilinear theory, is in principle available, and can therefore be applied to the beam–plasma system. Numerical solutions of the weak turbulence equation can then be compared in detail with simulation results. However, to this date, no attempts have been made to systematically solve the full set of self-consistent weak turbulence kinetic equations. Instead, certain nonlinear processes are presumed to dominate *a priori*, and terms which reflect other processes are then discarded at the outset. For instance, Refs. 32–35 focus on the wave–wave interactions, while Refs. 36–38 only emphasize the nonlinear wave–particle interactions.

Of course, weak turbulence theory cannot describe coherent nonlinear processes such as particle trapping which were thought to be the primary saturation mechanism of beam–plasma instability in the early days. This was largely motivated by early simulation results [39,40] and to some extent by laboratory experiments,[41–45] many of which were specifically designed to test the very trapping phenomenon. However, depending on the physical parameters and initial setup,

[a)]Electronic mail: ziebell@if.ufrgs.br
[b)]Electronic mail: rudi@ufpel.tche.br
[c)]Electronic mail: yoonp@ipst.umd.edu

numerical simulations[39,46–55] or laboratory experiments[56–60] can produce results that are in good overall agreement with incoherent turbulence theory. Specifically, for a very cold or intense beam, the trapping can become significant, at least in the early stage, but for a weak beam the weak turbulence approach is now known to reliably describe the instability development.

In this regard, it is noteworthy that, on the basis of renormalized kinetic theory, some serious questions on the validity of quasilinear theory were raised in the 1980's.[61–63] In particular, it was argued that the so-called turbulent particle trapping leads to a significant modification of quasilinear theory which invalidates the quasilinear approximation which constitutes a lowest-order theory in the weak turbulence perturbation scheme. However, subsequent experimental and simulation efforts to verify the theoretical claim that turbulent trapping should lead to a significant increase of the velocity–space diffusion rate, failed to produce definitive results.[60,64,65]

Almost a decade had passed when Liang and Diamond[66] carried out a correct renormalized kinetic analysis to show that the effects due to turbulent trapping on the velocity–space diffusion is insignificantly small, thus reestablishing the validity of quasilinear theory. Meanwhile, on the basis of carefully designed numerical simulations, Dum[51] demonstrated that early simulations which showed wave trapping as a dominant saturation mechanism were largely due to a small simulation size and insufficient mode resolution. Dum's simulations showed that the wave trapping is but a transient phenomenon, a finding in agreement with experimental findings by Dimonte and Malmberg,[59] for instance. Dum also pointed out the significance of backscattering of primary Langmuir waves by the ions, which is one of the processes described by weak turbulence theory. Muschietti and Dum[38] then solved a simplified weak turbulence equation in which terms depicting only the quasilinear process and induced scattering off ions are kept while the decay process is ignored. However, to this date, the relative roles and importance of induced scattering off ions versus the three-wave decay process are not completely resolved. Recently, Cairns[68] discusses the issue of the roles played by the decay versus scattering processes, which are the two main nonlinear processes in the context of weak turbulence theory. However, since the discussion by Cairns is based upon purely analytical means, one cannot demonstrate the effects of the two processes in a quantifiable manner.

Our purpose in the present paper is to solve the full set of conventional weak turbulence kinetic equations for the first time, and to examine the roles of various wave–wave and wave–particle interactions in beam–plasma interaction processes. The structure of the paper is the following: In Sec. II we formulate the theoretical equations to be numerically analyzed in detail. In Sec. III we conduct the numerical computation of the equations. Finally, some comments on the results obtained and on the perspectives for future work appear in Sec. IV.

II. THEORETICAL FRAMEWORK

We start from the formulation derived in Ref. 67, which is valid for electrostatic interactions only, ignoring the effects of thermal fluctuations and an ambient magnetic field. In the present analysis, we only retain those terms in the generalized kinetic equations derived in Ref. 67 that are commonly found in the conventional weak turbulence theory. It includes the contribution of Langmuir (L) and ion-sound (S) waves. From Eqs. (16), (18), and (23) of Ref. 67, which reduce to the well-known equations of conventional weak turbulence theory[18–31] if we ignore the harmonic nonlinear eigenmode, the dynamics of Langmuir waves is governed by the following equation:[68,69]

$$\begin{aligned}\frac{\partial I_{\mathbf{k}}^{\sigma L}}{\partial t} &= \sigma\omega_{\mathbf{k}}^{L}\int d\mathbf{v}\Gamma_{\mathbf{k}}^{L}\mathbf{k}\cdot\frac{\partial F_e}{\partial \mathbf{v}} I_{\mathbf{k}}^{\sigma L} \\ &+ \sum_{\sigma',\sigma''=\pm 1}\sigma\omega_{\mathbf{k}}^{L}\int d\mathbf{k}' V_{\mathbf{k},\mathbf{k}'}^{L}\left[\sigma\omega_{\mathbf{k}}^{L} I_{\mathbf{k}'}^{\sigma' L} I_{\mathbf{k}-\mathbf{k}'}^{\sigma'' S}\right. \\ &\left. -(\sigma'\omega_{\mathbf{k}'}^{L} I_{\mathbf{k}-\mathbf{k}'}^{\sigma'' S}+\sigma''\omega_{\mathbf{k}-\mathbf{k}'}^{L} I_{\mathbf{k}'}^{\sigma' L}) I_{\mathbf{k}}^{\sigma L}\right] \\ &- \sum_{\sigma'=\pm 1}\int d\mathbf{k}'\int d\mathbf{v}\, U_{\mathbf{k},\mathbf{k}'}(\mathbf{k}-\mathbf{k}')\cdot\frac{\partial}{\partial \mathbf{v}} \\ &\times\left((\sigma\omega_{\mathbf{k}}^{L}-\sigma'\omega_{\mathbf{k}'}^{L})F_e-\frac{m_e}{m_i}(\sigma\omega_{\mathbf{k}}^{L})F_i\right) I_{\mathbf{k}'}^{\sigma' L} I_{\mathbf{k}}^{\sigma L},\end{aligned} \tag{1}$$

where $\sigma=\pm 1$ represents waves with phase velocities $\mathbf{v}_\varphi=\sigma\omega_{\mathbf{k}}/\mathbf{k}$, F_e and F_i are the electron and ion distributions, $\omega_{\mathbf{k}}$ and $\mathbf{k}$ are the wave angular frequency and wave vector, respectively, ω_{pe} and ω_{pi} are the electron and ion plasma angular frequencies, defined by $\omega_{pj}^2=4\pi n_0 e_j^2/m_j$, m_e and m_i being the electron and ion masses, n_0 the equilibrium electron density, and e the absolute value of the electron charge. The various coefficients in Eq. (1) are given by

$$\begin{aligned}\Gamma_{\mathbf{k}}^{L} &= \pi\frac{\omega_{pe}^2}{k^2}\delta(\sigma\omega_{\mathbf{k}}^{L}-\mathbf{k}\cdot\mathbf{v}), \\ V_{\mathbf{k},\mathbf{k}'}^{L} &= \frac{\pi}{2}\frac{e^2}{T_e^2}\frac{\mu_{\mathbf{k}-\mathbf{k}'}(\mathbf{k}\cdot\mathbf{k}')^2}{k^2 k'^2|\mathbf{k}-\mathbf{k}'|^2} \\ &\quad\times\delta(\sigma\omega_{\mathbf{k}}^{L}-\sigma'\omega_{\mathbf{k}'}^{L}-\sigma''\omega_{\mathbf{k}-\mathbf{k}'}^{S}), \\ U_{\mathbf{k},\mathbf{k}'} &= \frac{\pi}{\omega_{pe}^2}\frac{e^2}{m_e^2}\frac{(\mathbf{k}\cdot\mathbf{k}')^2}{k^2 k'^2}\delta[\sigma\omega_{\mathbf{k}}^{L}-\sigma'\omega_{\mathbf{k}'}^{L}-(\mathbf{k}-\mathbf{k}')\cdot\mathbf{v}], \\ \mu_{\mathbf{k}} &= |k|^3\lambda_{De}^3(m_e/m_i)^{1/2}(1+3T_i/T_e)^{1/2},\end{aligned} \tag{2}$$

where $\lambda_{De}^2=T_e/4\pi n_0 e^2$ is the square of the electron Debye length.[70]

The first term on the right-hand side of Eq. (1) which contains the delta function, $\delta(\sigma\omega_{\mathbf{k}}-\mathbf{k}\cdot\mathbf{v})$, depicts the induced (or stimulated) emission/absorption, or equivalently, the bump-on-tail instability linear growth/Landau damping. Obviously, this process is dictated by resonant linear wave-particle interaction. The second term on the right-hand side represents the nonlinear three-wave decay process, which

preserves the frequency and wave number matching condition between two Langmuir waves and an ion-sound wave, as the delta function condition, $\delta(\sigma\omega^L_{\mathbf{k}}-\sigma'\omega^L_{\mathbf{k}'}-\sigma''\omega^S_{\mathbf{k}-\mathbf{k}'})$, indicates. Finally, the third term on the right-hand side dictated by the factor $\delta[\sigma\omega^L_{\mathbf{k}}-\sigma'\omega^L_{\mathbf{k}-\mathbf{k}'}-(\mathbf{k}-\mathbf{k}')\cdot\mathbf{v}]$, describes the induced (or stimulated) scattering of Langmuir waves off particles. The induced scattering off the electrons (i.e., the first term within the large parantheses which involves F_e) is called the nonlinear Landau damping in early literatures. The same nonlinear wave–particle interaction process involving the ions is termed "the scattering off ions," or generalized nonlinear Landau damping off ions.

The ion-sound wave kinetic equation is given by

$$\frac{\partial I^{\sigma S}_{\mathbf{k}}}{\partial t}=\sigma\omega^L_{\mathbf{k}}\int d\mathbf{v}\Gamma^S_{\mathbf{k}}\mathbf{k}\cdot\frac{\partial}{\partial\mathbf{v}}\left(F_e+\frac{m_e}{m_i}F_i\right)I^{\sigma S}_{\mathbf{k}}$$
$$+\sum_{\sigma',\sigma''=\pm1}\sigma\omega^L_{\mathbf{k}}\int d\mathbf{k}'\,V^S_{\mathbf{k},\mathbf{k}'}[\,\sigma\omega^L_{\mathbf{k}}I^{\sigma' L}_{\mathbf{k}'}I^{\sigma'' L}_{\mathbf{k}-\mathbf{k}'}$$
$$-(\sigma'\omega^L_{\mathbf{k}'}I^{\sigma'' L}_{\mathbf{k}-\mathbf{k}'}+\sigma''\omega^L_{\mathbf{k}-\mathbf{k}'}I^{\sigma' L}_{\mathbf{k}'})I^{\sigma S}_{\mathbf{k}}],$$

$$\Gamma^S_{\mathbf{k}}=\pi\,\mu_{\mathbf{k}}\frac{\omega^2_{pe}}{k^2}\delta(\sigma\omega^S_{\mathbf{k}}-\mathbf{k}\cdot\mathbf{v}),$$

$$V^S_{\mathbf{k},\mathbf{k}'}=\frac{\pi}{4}\frac{e^2}{T_e^2}\frac{\mu_{\mathbf{k}}[\mathbf{k}'\cdot(\mathbf{k}-\mathbf{k}')]^2}{k^2k'^2|\mathbf{k}-\mathbf{k}'|^2}$$
$$\times\delta(\sigma\omega^S_{\mathbf{k}}-\sigma'\omega^L_{\mathbf{k}'}-\sigma''\omega^L_{\mathbf{k}-\mathbf{k}'}). \tag{3}$$

In Eqs. (1) and (3), we have modified the definition of the ion-sound wave intensity $I^S_{\mathbf{k}}$, as compared to that appearing in Ref. 67, by dividing it by factor $\mu_{\mathbf{k}}$, $I^S_{\mathbf{k}}\rightarrow I^S_{\mathbf{k}}/\mu_{\mathbf{k}}$. Accordingly, we have redefined the various coefficients, $V^L_{\mathbf{k},\mathbf{k}'}$, $U_{\mathbf{k},\mathbf{k}'}$, etc.

For the electron dynamics, following the standard methods as found in the conventional weak turbulence theory, we utilize the usual quasilinear approximation, which ignores the effects of nonlinear wave–particle interactions on the particles. Moreover, we only incorporate the wave–particle resonance between the electrons and Langmuir waves. From Eq. (42) of Ref. 67, we thus obtain

$$\frac{\partial F_e}{\partial t}=\frac{\partial}{\partial v_i}\left(D_{ij}\frac{\partial F_e}{\partial v_j}\right), \tag{4}$$

where

$$D_{ij}=\frac{\pi e^2}{m_e^2}\int d\mathbf{k}\frac{k_i k_j}{k^2}\sum_{\sigma=\pm1}\delta(\sigma\omega^L_{\mathbf{k}}-\mathbf{k}\cdot\mathbf{v})\,I^{\sigma L}_{\mathbf{k}}. \tag{5}$$

For the ion distribution, we assume a constant Maxwellian distribution with thermal speed, $v_i=(2T_i/m_i)^{1/2}$.

At this point, we should point out that the three-wave decay coefficients, $V^L_{\mathbf{k},\mathbf{k}'}$ and $V^S_{\mathbf{k},\mathbf{k}'}$, and the coefficient for the induced scattering, $U_{\mathbf{k},\mathbf{k}'}$, as defined in Eqs. (1)–(3), are based upon a number of approximations.[67] However, in principle, more general expressions of these quantities in terms of various linear response functions are available. These are

$$V^L_{\mathbf{k},\mathbf{k}'}=\frac{\pi}{4\omega^4_{pe}}\frac{e^2}{m_e^2}\frac{\mu_{\mathbf{k}-\mathbf{k}'}(\mathbf{k}\cdot\mathbf{k}')^2}{k^2k'^2}|\mathbf{k}-\mathbf{k}'|^2$$
$$\times|\chi_e(\mathbf{k}-\mathbf{k}',\sigma\omega^L_{\mathbf{k}}-\sigma'\omega^L_{\mathbf{k}'})|^2$$
$$\times\delta(\sigma\omega^L_{\mathbf{k}}-\sigma'\omega^L_{\mathbf{k}'}-\sigma''\omega^S_{\mathbf{k}-\mathbf{k}'}),$$

$$V^S_{\mathbf{k},\mathbf{k}'}=\frac{\pi}{4\omega^4_{pe}}\frac{e^2}{m_e^2}\frac{\mu_{\mathbf{k}}[\mathbf{k}'\cdot(\mathbf{k}-\mathbf{k}')]^2}{k'^2|\mathbf{k}-\mathbf{k}'|^2}k^2|\chi_e(\mathbf{k},\sigma\omega^S_{\mathbf{k}})|^2$$
$$\times\delta(\sigma\omega^S_{\mathbf{k}}-\sigma'\omega^L_{\mathbf{k}'}-\sigma''\omega^L_{\mathbf{k}-\mathbf{k}'})$$

and

$$U_{\mathbf{k},\mathbf{k}'}=\frac{\pi}{\omega^2_{pe}}\frac{e^2}{m_e^2}\frac{(\mathbf{k}\cdot\mathbf{k}')^2}{k^2k'^2}$$
$$\times\frac{[\,\mathrm{Re}\,\chi_e(\mathbf{k}-\mathbf{k}',\sigma\omega^L_{\mathbf{k}}-\sigma'\omega^L_{\mathbf{k}'})\,]^2}{|\epsilon(\mathbf{k}-\mathbf{k}',\sigma\omega^L_{\mathbf{k}}-\sigma'\omega^L_{\mathbf{k}'})|^2}$$
$$\times\delta[\sigma\omega^L_{\mathbf{k}}-\sigma'\omega^L_{\mathbf{k}'}-(\mathbf{k}-\mathbf{k}')\cdot\mathbf{v}],$$

where $\epsilon(\mathbf{k},\omega)=1+\chi_e(\mathbf{k},\omega)+\chi_i(\mathbf{k},\omega)$ is the linear dielectric response function. In the literature, the general expressions such as given above are sometimes used for the induced-scattering coefficient.[38] However, in the discussion of the three-wave decay process in the literature, the simplified versions of $V^L_{\mathbf{k},\mathbf{k}'}$ and $V^S_{\mathbf{k},\mathbf{k}'}$ as defined in Eqs. (2) and (3) are used invariably. For the sake of simplicity and internal consistency, we resort to the simplified expressions for $V^L_{\mathbf{k},\mathbf{k}'}$ and $V^S_{\mathbf{k},\mathbf{k}'}$, and $U_{\mathbf{k},\mathbf{k}'}$ throughout the present analysis.

In what follows, we simplify the analysis by considering a one-dimensional limit where both the particles and the excited waves propagate either in the same direction or in exactly opposite directions with respect to each other. We proceed by defining the following nondimensional quantities:

$$z\equiv\omega/\omega_{pe},\quad q\equiv kv_e/\omega_{pe},\quad \tau\equiv\omega_{pe}t,\quad u\equiv v/v_e, \tag{6}$$

where $v_e^2=2T_e/m_e$, and we define the normalized distributions, $F_e(u)$ and $F_i(u)$, such that $\int du\,F_e(u)=\int dv\,F_e(v)$, $\int du\,F_i(u)=\int dv\,F_i(v)$. We also define the nondimensional wave intensity I_q, such that

$$\frac{1}{8\pi n_0T_e}\int dk\,I_k=\int dq\,I_q. \tag{7}$$

The dispersion relations for the L and S waves are obtained by considering the bulk of the distribution function. For the Langmuir waves, the familiar dispersion relation $\omega^L_k=\omega_{pe}(1+3k^2\lambda^2_{\mathrm{De}})^{1/2}$ reduces to the normalized form

$$z^L_q=(1+3q^2/2)^{1/2}\simeq1+3q^2/4, \tag{8}$$

while the ion-sound wave dispersion relation $\omega^S_k=kc_S(1+3T_i/T_e)^{1/2}/(1+k^2\lambda^2_{\mathrm{De}})^{1/2}$ becomes

$$z^S_q=qA\,(1+q^2/2)^{-1/2}\simeq qA, \tag{9}$$

where

$$A\equiv\frac{1}{\sqrt{2}}\left(\frac{m_e}{m_i}\right)^{1/2}\left(1+\frac{3T_i}{T_e}\right)^{1/2}. \tag{10}$$

In approximating the ion-sound dispersion relation (9), it has been assumed that the wave spectra are significant only for q sufficiently less than unity.

Muschietti and Dum[38] discuss the effects of the more general Langmuir wave dispersion relation obtained from the full dispersion equation rather than the simplified expression (8), z_q^L, which is a monotonically increasing function of q. They discuss that the use of more general numerically computed dispersion relation results in a significant quantitative different in the induced scattering process. In this sense, Ref. 38 is more general than our approach. However, since their study ignores the decay process at the outset, it is difficult to assess the effects of adopting the same numerical dispersion relation on the decay process.

The electron quasilinear diffusion equation in the normalized form is given by

$$\frac{\partial F_e}{\partial \tau}=\frac{\partial}{\partial u}\left(\frac{2\pi}{|u|}[\Theta(u)(I_q^{+L})_{q=1/|u|}+\Theta(-u)(I_q^{-L})_{q=1/|u|}]\frac{\partial F_e}{\partial u}\right). \tag{11}$$

The ions remain stationary, with the distribution function in normalized form given by

$$F_i(u)=\frac{1}{\sqrt{\pi}}\left(\frac{m_i}{m_e}\frac{T_e}{T_i}\right)^{1/2}\exp\left(-\frac{m_i}{m_e}\frac{T_e}{T_i}u^2\right). \tag{12}$$

After various u integrals are explicitly performed by virtue of the delta function resonance conditions, paying careful attention to all possible signs of $(\sigma,\sigma',\sigma'')$, the resulting nondimensionalized set of kinetic equations are given by the subsequent expressions. First, the forward- and backward-propagating Langmuir wave kinetic equations ($\sigma=1$, and defined in the positive q domain) are given, respectively, by

$$\begin{aligned}\frac{\partial I_q^{\pm L}}{\partial \tau}=&\pm\frac{\pi z_q^L}{q^2}\left(\frac{\partial F_e}{\partial u}\right)_{u=\pm z_q^L/q} I_q^{\pm L}+\pi\Theta(q-\eta)\,\eta\, z_q^L[z_q^L I_{q-\eta}^{\mp L}I_{2q-\eta}^{\pm S}-(z_{q-\eta}^L I_{2q-\eta}^{\pm S}+z_{2q-\eta}^L I_{q-\eta}^{\mp L})I_q^{\pm L}]\\
&+\pi\,\eta\, z_q^L[z_q^L I_{q+\eta}^{\mp L}I_{2q+\eta}^{\mp S}-(z_{q+\eta}^L I_{2q+\eta}^{\mp S}-z_{2q+\eta}^L I_{q+\eta}^{\mp L})I_q^{\pm L}]\\
&+\pi\Theta(\eta-q)\Theta(2q-\eta)\,\eta\, z_q^L[z_q^L I_{\eta-q}^{\pm L}I_{2q-\eta}^{\pm S}-(z_{\eta-q}^L I_{2q-\eta}^{\pm S}+z_{2q-\eta}^L I_{\eta-q}^{\pm L})I_q^{\pm L}]\\
&+\pi\Theta(\eta-q)\Theta(\eta-2q)\,\eta\, z_q^L[z_q^L I_{\eta-q}^{\pm L}I_{\eta-2q}^{\pm S}-(z_{\eta-q}^L I_{\eta-2q}^{\pm S}-z_{\eta-2q}^L I_{\eta-q}^{\pm L})I_q^{\pm L}]\\
&\mp\pi\int_0^\infty dq'|q+q'|\,u\left(\frac{\partial F_e}{\partial u}+\frac{2T_e}{T_i}\frac{z_q^L}{q+q'}F_i\right)_{u=\pm 3(q-q')/4} I_{q'}^{\mp L}I_q^{\pm L}\\
&\mp\pi\int_0^\infty dq'|q-q'|\,u\left(\frac{\partial F_e}{\partial u}+\frac{2T_e}{T_i}\frac{z_q^L}{q-q'}F_i\right)_{u=\pm 3(q+q')/4} I_{q'}^{\pm L}I_q^{\pm L},\end{aligned} \tag{13}$$

where

$$\eta\equiv 4A/3. \tag{14}$$

For ion-sound waves, the resulting equation for forward- and backward-propagating components are given, respectively, by

$$\begin{aligned}\frac{\partial I_q^{\pm S}}{\partial \tau}=&\pm\frac{3\pi}{8}\,\eta\, z_q^L q\left(\frac{\partial F_e}{\partial u}-\frac{T_e}{T_i}(2uF_i)\right)_{u=\pm z_q^S/q} I_q^{\pm S}\\
&+\frac{\pi}{2}\Theta(\eta-q)\,\eta\, z_q^L[z_q^L I_{(\eta-q)/2}^{\pm L}I_{(q+\eta)/2}^{\pm L}\\
&+(z_{(\eta-q)/2}^L I_{(q+\eta)/2}^{\pm L}-z_{(q+\eta)/2}^L I_{(\eta-q)/2}^{\pm L})I_q^{\pm S}]\\
&+\frac{\pi}{2}\Theta(q-\eta)\,\eta\, z_q^L[z_q^L I_{(q+\eta)/2}^{\pm L}I_{(q-\eta)/2}^{\mp L}\\
&-(z_{(q+\eta)/2}^L I_{(q-\eta)/2}^{\mp L}-z_{(q-\eta)/2}^L I_{(q+\eta)/2}^{\pm L})I_q^{\pm S}].\end{aligned} \tag{15}$$

III. NUMERICAL ANALYSIS

Equations (13)–(15), together with Eq. (11), form a coupled system of equations which we have solved using a fifth-order Runge–Kutta method.[71] For the application which follows, we used the velocity and wave number ranges corresponding to $-15<u<15$, and $1\times10^{-6}<q<0.5$, respectively (or $-0.5<q<0.5$ if we convert the q-range corresponding to the backward propagating waves into a negative q-range by virtue of the symmetry relation, $I_q^{-\sigma}=I_{-q}^{-\sigma}$, $\sigma=L,S$).

In the present formalism which ignores the spontaneous thermal fluctuations, the choice of initial level and functional form of the wave spectrum are somewhat arbitrary. In a complete theory in which spontaneous effects are included, the issue of the initial wave level and spectral form would matter less because, to a certain extent, the contribution from the spontaneous emission to the initial wave level and spectral shape is expected to be of primary importance. Such a theory is, of course, available in the literature.[22,27,29,30] As a matter of fact, Ref. 38, for instance, incorporates just such an effect in its numerical study of weak Langmuir turbulence.

In the present analysis, however, we do not include such

an effect. The reason is that the present analysis actually forms the first part in a two-part series. The second part, which is forthcoming, deals with the numerical solution of the generalized weak turbulence theory[67] in which the harmonic Langmuir wave is included as part of the eigenmode system. For such a problem, however, there is no readily-available theory which includes the effects of spontaneously generated fluctuations. Therefore, for the purpose of a comparison between the conventional treatment of weak Langmuir turbulence, and the general treatment including the harmonic Langmuir mode, it is better to ignore the spontaneous fluctuations in both cases. Obviously, in the future studies the present simplifications must be removed.

In any case, for the present situation, we chose the initial wave level to be constant over the range $1\times10^{-6}<q<0.5$ for both the forward and backward propagating L and S waves. The specific functional form for the initial spectrum is not expected to matter too much, since the waves in the unstable range will be amplified while the damped portion of the spectrum will exponentially decrease shortly after the initial stage anyway. However, the magnitude of the initial spectrum does matter greatly, as we will see. To discuss the effects of the initial wave amplitude, we have considered two levels of initial normalized intensity, $I_q(0)=2\times10^{-4}$ and $I_q(0)=5\times10^{-4}$, for q in the range $1\times10^{-6}<q<0.5$.

For the initial electron distribution, we have assumed a combination of a Maxwellian distribution and a drifting Maxwellian,

$$F_e(0)=\left(1-\frac{n_b}{n_0}\right)\frac{\exp(-u^2)}{\sqrt{\pi}}+\frac{n_b}{n_0}\frac{1}{\sqrt{\pi}\,\alpha_b}\times\exp\left[-\frac{(u-u_b)^2}{\alpha_b^2}\right]. \tag{16}$$

The number density ratio of the beam to background electrons, n_b/n_0, is a highly relevant parameter. We have taken into account a couple of considerations in the choice of n_b/n_0. First, although in this article we address generic plasma physics issues associated with the beam–plasma instability, we are nevertheless concerned with physical situations in the solar wind and interplanetary space, where n_b/n_0 is very low (as a matter of fact, it is often said that the solar and interplanetary application of a beam–plasma interaction is perhaps the ideal case where the weak turbulence theory is entirely applicable). Second, the simulated computer experiments of beam–plasma instability have many practical difficulties in dealing with very low n_b/n_0. However, the present theory does not suffer from typical numerical and computer resource problems. Therefore, we have chosen to consider a situation which has not been considered in numerical studies of beam–plasma instability before. Specifically, we choose the value of $n_b/n_0=2\times10^{-4}$.

Other parameters are the normalized average beam speed, u_b, the ratio of beam velocity spread to background thermal speed, α_b, and the electron-to-ion temperature ratio, T_e/T_i. Of course, the ion-to-electron mass ratio is given by the real value $m_i/m_e=1836$. This is another advantage of the present approach, as the true-mass ratio computer simulations are notoriously difficult. Of these parameters, we choose $u_b=5.0$ and $\alpha_b=1.0$. In the numerical analysis to follow, for the sake of simplicity and the length of the article, we do not vary these parameters. However, the temperature ratio T_e/T_i is an important parameter, hence we consider four possible choices, $T_e/T_i=4$, 7, 10, and 14. The reason T_e/T_i is considered to be important is that the three-wave decay process involves ion-sound waves which are heavily damped unless this parameter is sufficiently high. In the literature it is often said that when T_e/T_i is low, then the induced scattering should dominate, while for reasonably high T_e/T_i, the decay process should be more important than the induced scattering process.[68] As a reference, the value of T_e/T_i in the solar wind is approximately 4, for which the ion-sound damping rate should be marginal. The choice of $T_e/T_i=7$ is already unrealistically high for the solar wind. We nevertheless considered T_e/T_i up to 14 in order to assess the importance of this parameter in the nonlinear process. For the majority of the discussions on numerical analysis, however, we have considered an intermediate value, $T_e/T_i=7$.

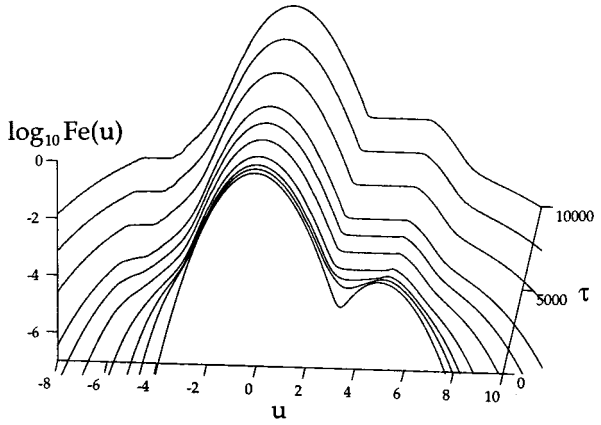

FIG. 1. A plot of electron distribution function, $F_e(u,\tau)$, vs u and τ, for the case of $n_b/n_0=2\times10^{-4}$, $u_b=5$, $T_e/T_i=7$, and with an initial wave level of $I_q^L(0)=I_q^S(0)=2\times10^{-4}$.

In Fig. 1, we plot the electron distribution function, $F_e(u,\tau)$, in the logarithmic vertical scale versus u and τ, for $n_b/n_0=2\times10^{-4}$, $u_b=5$, $\alpha_b=1$, $I_q^L(0)=I_q^S(0)=2\times10^{-4}$, and $T_e/T_i=7$. We have plotted the distribution $F_e(u,\tau)$ at time intervals corresponding to $\tau=0$, 250, 500, 10^3, 2×10^3, 3×10^3, 4×10^3, 6×10^3, 8×10^3, and 10^4. The relatively early-time development of $F_e(u,\tau)$ is as expected from the usual quasilinear diffusion theory. We observe that the bump-on-tail feature quickly develops into a plateau by the time the system has evolved to $\tau\approx2\times10^3$ or so. It is interesting to note that for a sufficiently long time, τ beyond 6000 or so, the electrons are seen to develop an energetic tail, and that the electron distribution in the negative u range develops a mini plateau, somewhat similar to the plateau on the positive u side. This is intimately related to the generation of backscattered Langmuir waves by the combined decay and scattering processes, as will be discussed below.

Of particular interest is the development of wave intensity spectra. In Fig. 2, we plot Langmuir and ion-sound wave

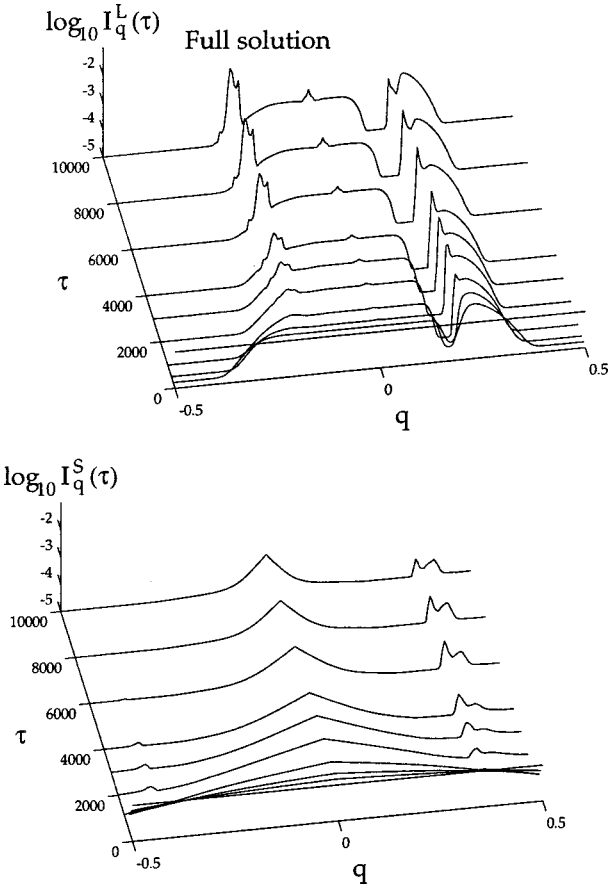

FIG. 2. A plot of Langmuir wave intensity, $I_q^L(\tau)$, and ion-sound wave intensity, $I_q^S(\tau)$, vs q and τ, for the case of $n_b/n_0=2\times10^{-4}$, $u_b=5$, $T_e/T_i=7$, and with an initial wave level of $I_q^L(0)=I_q^S(0)=2\times10^{-4}$. This plot corresponds to the solution of a complete wave kinetic equation including the induced emission (quasilinear), decay (three-wave interaction), and induced-scattering terms.

intensity spectra, $I_q^L(\tau)$ and $I_q^S(\tau)$, corresponding to the same run as in Fig. 1, in logarithmic vertical scaled versus q and τ. In Fig. 2, to aid the visual representation, we have added a small constant $\epsilon=1\times10^{-5}$ to the spectra. As a result, the actual quantity plotted are $\log_{10}[I_q^L(\tau)+\epsilon]$ and $\log_{10}[I_q^S(\tau)+\epsilon]$. The horizontal lines at $\tau=0$ correspond to the initially constant wave intensities. The portion of spectra corresponding to positive q belongs to the forward components, $I_q^{+L}(\tau)$ and $I_q^{+S}(\tau)$, while the negative q regions are for the backward components, $I_q^{-L}(\tau)$ and $I_q^{-S}(\tau)$. For relatively early times, one can see that, depending on the spectral range, the initially constant wave spectra quickly damp out, stay constant, or get amplified. Note that the linear bump-on-tail instability theory predicts a maximum growth rate around $q\approx1/u_b=1/5=0.2$. In accordance with such a prediction, the Langmuir mode initially grows exponentially for q around 0.2. For later times ($\tau\sim2\times10^3$ or so), one can observe that the long-wavelength Langmuir mode (near $q\approx0$) and the backscattered L mode ($q\approx-0.2$) begin to grow as a result of nonlinear processes. Meanwhile, the ion-sound waves continuously damp out almost everywhere, except near $q\sim0$ and $q\sim0.4$.

To analyze the various nonlinear processes involved in the beam–plasma instability development, we have considered various terms in the wave kinetic equations one at a time. Of first and foremost importance is the quasilinear process—that is, the induced emission/absorption, or equivalently, the bump-on-tail growth and Landau damping. In Fig. 3, we present the result of the numerical computation of $F_e(u)$ and $I_q^L(\tau)$ in which both the decay and induced-scattering terms are turned off artificially, and only the quasilinear terms are kept. In this case, the ion-sound waves do not participate in the process, and thus the spectral intensity $I_q^S(\tau)$ is not shown. The result is as expected from the classic quasilinear theory in that the linear exponential growth is followed by a saturation stage, while the damped portion of the initial wave spectrum exponentially damps out. The narrow peak in the Langmuir wave spectrum is the result of a small remnant positive gradient in the beam electron distribution, $F_e(u)$, which persists for awhile (see Fig. 1 near the high-velocity edges of the velocity plateau for $\tau=10^3$, 2×10^3, and 3×10^3). The persistence of the gradient in $F_e(u)$ seems to be the result of quasilinear diffusion approximation which we adopted for the electrons.

It is interesting to note that although the initial beam feature disappears as a result of plateau formation and thus the quasilinear wave–particle interaction process should no longer be effective, the bulk of the electrons nevertheless appear to be heated and the energetic tail is seen to form. The overall feature associated with the energetic tail in the late phase of electron distribution development is qualitatively similar to that seen in the full solution, Fig. 1. This can be explained by the fact that although linear beam–plasma instability is quenched by the time the plateau has fully developed, the initially imposed waves are continually absorbed by the bulk plasma through a Landau damping process. Note, however, that the mini plateau structure in $F_e(u)$ for $u<0$ is absent in the present quasilinear solution, and that the distribution features rather smooth profiles over the entire negative u range. On the basis of Fig. 3, we thus conclude that while the gross characteristics of beam–plasma instability as shown by the evolutions of electron distribution function and spectral intensities shown in Fig. 2 can be understood in terms of zeroth-order quasilinear theory, the peaks at $q\sim0$ and $q\sim-0.2$ in the Langmuir wave spectrum, the generation of ion-sound waves, and the plateau associated with negative velocities in the bulk electron distribution function must be due to nonlinear processes.

To understand the origin of the long-wavelength modes at $q\sim0$, the backscattered component near $q\sim-0.2$, as well as the nature of negative-u plateau, we have then considered the wave kinetic equations for L and S waves in which only the quasilinear terms and the terms due to three-wave decay process are kept in the wave kinetic equations, but in which the terms corresponding to induced-scattering processes are artificially ''turned off.'' The solution of such equations are displayed in Figs. 4 and 5. First, as expected, the time development of the electron distribution is very similar to that of Fig. 1 or that shown in Fig. 3 in an overall sense. However, unlike the quasilinear case, the late-time behavior of $F_e(u)$, especially the negative-u plateau formation, closely resembles that of Fig. 1, which indicates that the detailed struc-

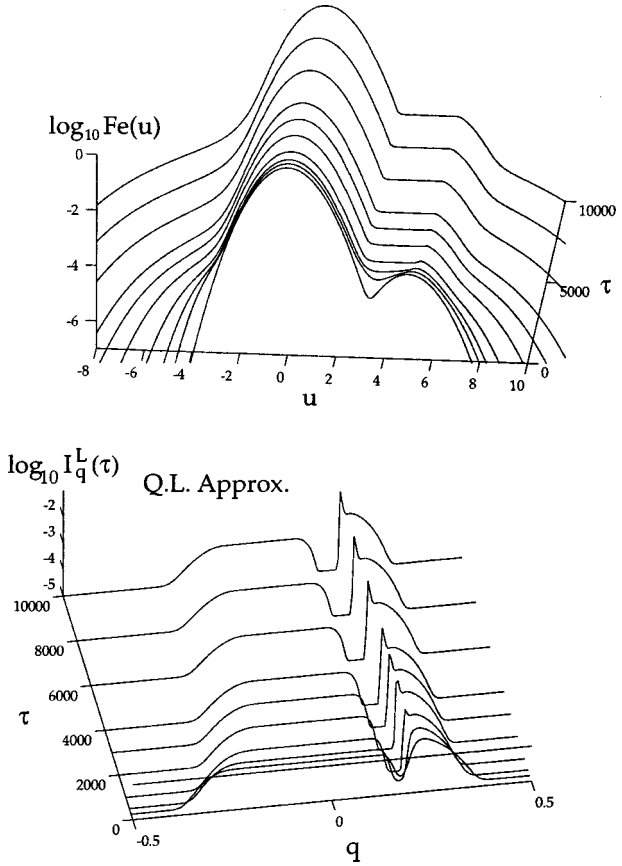

FIG. 3. A plot of electron distribution function, $F_e(u,\tau)$, vs u and τ, and Langmuir wave intensity $I_q^L(\tau)$, vs q and τ, in the same format as Figs. 1 and 2, except that this solution represents the classical quasilinear approximation, where both the three-wave and induced-scattering terms are ignored, and only an induced emission process is retained. The ion-sound waves do not participate in this process.

ture associated with the electron distribution for late times can be attributed to the quasilinear absorption of initial wave energy by the bulk electrons combined with the nonlinear wave-coupling process(es) which modifies the Langmuir wave spectrum, which in turn leads to the said negative-u plateau.

Second, we note that the ion-sound wave spectrum is qualitatively similar to that shown in Fig. 2, in that the spectral range of nonvanishing S-mode waves at a late phase, namely, $q\sim 0$ and $q\sim 0.4$, are in agreement with the full solution. This is to be expected since the physical processes which affect the ion-sound waves are linear damping and the three-wave decay process only, and that the ion-sound waves do not participate in the induced-scattering process. However, the detail spectral shape is appreciably different from the full solution which includes the induced-scattering process. This shows that the induced-scattering process, although it does not involve ion-sound waves directly, can nevertheless affect the excitation of S waves in an indirect manner, through the modification of forward and backward L-mode spectra, which in turn, enter the three-wave decay process.

Finally, the evolution of the L wave shows that the decay process affects the spectrum of the Langmuir waves quite

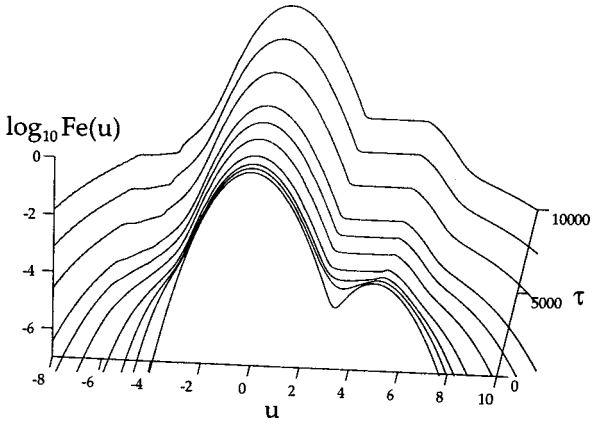

FIG. 4. A plot of electron distribution $F_e(u)$ in the same format as Fig. 1, except that only quasilinear and three-wave processes are considered. Induced scattering terms are ignored.

substantially. Specifically, the decay process leads to the generation of a backscattered Langmuir mode near $q\sim -0.2$ and the long-wavelength mode at $q\sim 0$, as in the full solution. Note that the primary Langmuir wave level decreases in the nonlinear stage, as the wave energy in the bump-on-tail mode is removed into the said long-wavelength mode and the backscattered L mode. By and large, the decay process

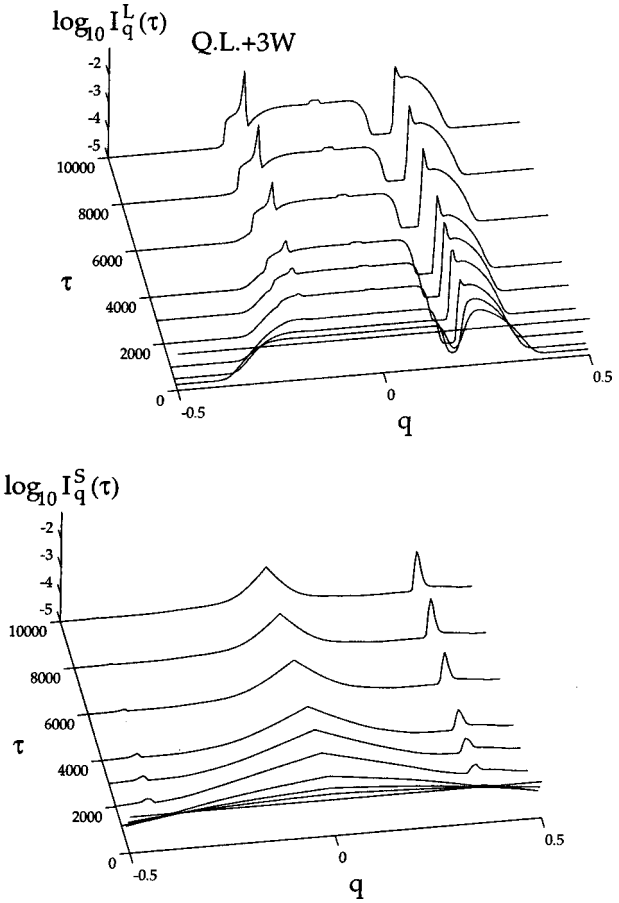

FIG. 5. A plot of Langmuir and ion-sound wave intensities in the same format as Fig. 2, except that only quasilinear and three-wave processes are considered. Induced-scattering terms are ignored.

appears to be quite effective in the generation of Langmuir and ion-sound modes in spectral ranges not accessible from the standpoint of linear theory.

The origin of $q\sim-0.2$ (backscattered) and $q\sim 0$ (long-wavelength) Langmuir modes produced by the decay process can be understood from Eq. (13), i.e., that the decay of primary Langmuir waves I_q^{+L} into product waves involves backward-propagating Langmuir waves, $I_{q\pm\eta}^{-L}$ and small q Langmuir waves with a wave number near $\eta\pm q$. From this, we see that the backscattered Langmuir waves with wave numbers equal to $q\pm\eta$, and the long-wavelength (small q) Langmuir waves with wave numbers $\eta\pm q$, are affected by the decay process.

Figure 6 displays the time evolution of the electron distribution $F_e(u)$ and Langmuir wave spectrum $I_q^L(\tau)$ when only the quasilinear and induced-scattering terms are kept in the wave kinetic equation. In this case, the three-wave decay terms are turned off, and thus, the ion-sound waves do not participate in the process. The induced-scattering process consists of two terms, one involving the electrons (nonlinear Landau damping) and the other, the ions (scattering off ions). Of the two processes, we found that the electron nonlinear Landau damping term is almost completely negligible, and that the induced scattering is dominated by the ions, which is in agreement with Ref. 37. According to Fig. 6, one can clearly see that the scattering off ions leads to the excitation of a long-wavelength Langmuir ($q\sim 0$) mode and the backscattered component ($q\sim-0.2$). The scattering of primary Langmuir waves into a long-wavelength mode near $q=0$ comes from the term with resonant velocities,

$$u=\pm 3(q+q')/4, \tag{17}$$

in Eq. (13), while the backscattering of a primary L wave into an oppositely traveling L wave originates from terms which involve resonant velocities,

$$u=\pm 3(q-q')/4. \tag{18}$$

The former condition can be understood from the fact that unless both q and q' are very small, such that $u=\pm 3(q+q')/4\ll 1$, the induced scattering cannot be effective. On the other hand, in order for the resonant velocity $u=\pm 3(q-q')/$ to remain small, q and q' must be almost equal. Since q' pertains to the backward L mode, this means that q' is almost equal but opposite in sign. The above consideration shows that the induced-scattering affects both $q\sim 0$ and ~-0.2 modes, just as the decay process does.

From the discussion thus far, one may conclude that both the decay process and the ion-scattering process operate in an overlapping spectral range and that both processes lead to the excitation of waves in spectral ranges that are not accessible by a linear wave–particle interaction process. The present result also shows that, in general, both the decay and scattering effects should be considered simultaneously, and that ignoring one process over the other may lead to quantitatively erroneous results.

To determine which of the two processes are more important in a relative sense,[68] we have made the comparisons among the three results at the final time $\tau=10^4$, that is, the full solution shown in Fig. 2, one in which only the decay process is kept among the wave-coupling terms, i.e., Fig. 4, and third, the one where only the scattering off ions are considered in the nonlinear terms, i.e., Fig. 6. To aid the readers, therefore, we have replotted in Fig. 7, the spectral wave intensities of the backscattered component, I_q^{-L}, and the primary Langmuir wave component, I_q^{+L}, in a linear vertical scale versus q (but to eliminate the jaggedness, we have interpolated the curves, so the results are much smoother than the previous figures), at the end of the computational time, $\tau=10^4$. The linear scale makes it clear that the approximate approach of retaining only the decay process is a poorer representation of the full solution when compared with the result obtained by the scheme in which only the scattering is retained. This result, therefore, shows that of the two processes, the decay process is less effective than the scattering off ions, although in general, one must retain both.

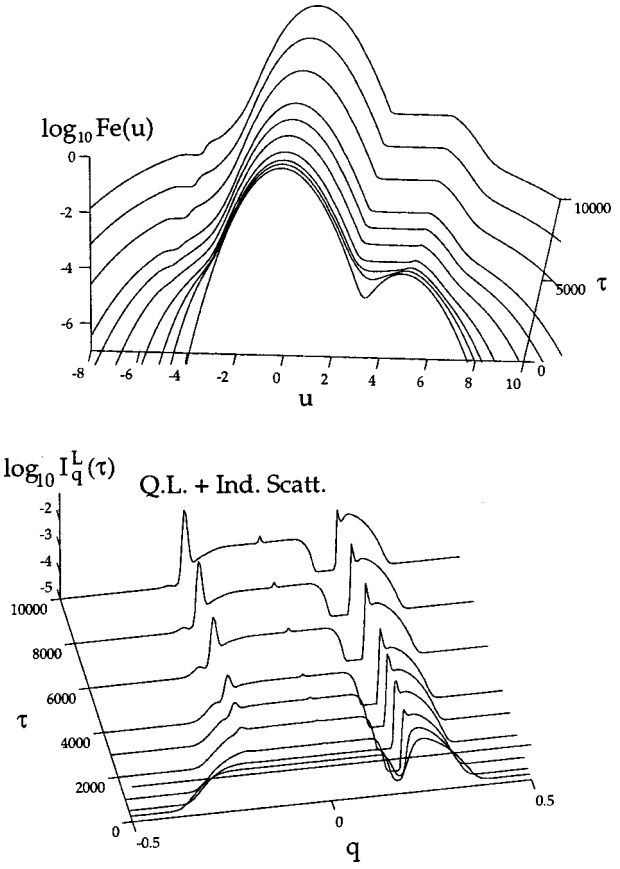

FIG. 6. A plot of electron distribution function, $F_e(u,\tau)$, vs u and τ, and Langmuir wave intensity $I_q^L(\tau)$, vs q and τ, in the same format as Figs. 1 and 2, except that in this solution only quasilinear and induced-scattering terms are retained, but three-wave interaction (decay) terms are ignored. The ion-sound waves do not participate in this process.

In view of the fact that the decay process is expected to be rather sensitive to the choice of electron-to-ion temperature ratio, T_e/T_i, we have considered various values of T_e/T_i other than the previous choice of $T_e/T_i=7$ to determine how sensitive the nonlinear processes are to the change in this parameter. According to the literature, T_e/T_i is one of the decisive parameters which determines the relative importance of the decay process versus the scattering. We have therefore considered three cases: $T_e/T_i=4$,10, and 14. The

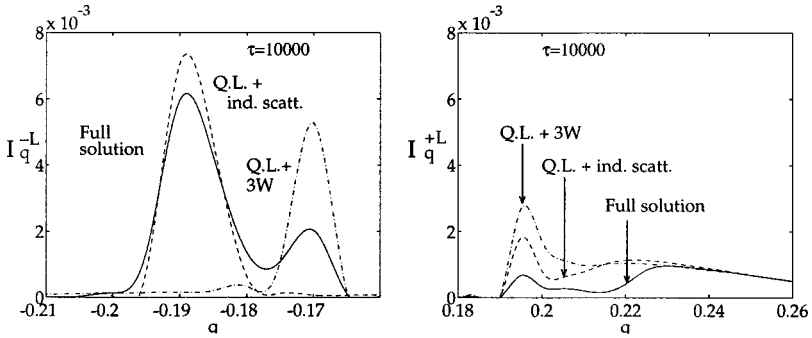

FIG. 7. A comparison of the full solution and the approximate solution in which only the quasilinear and induced scattering terms are included. A plot of the primary Langmuir wave intensity $I_q^{+L}(\tau)$, and backscattered Langmuir wave intensity $I_q^{-L}(\tau)$, vs q at $\tau=10^4$, shows that the approximate solution over-estimates the backscattered component while under-estimating the primary wave level.

results are displayed in Fig. 8. Other parameters are the same as in the previous case, namely, $n_b/n_0=2\times10^{-4}$, $I_q^L(0)=I_q^S(0)=2\times10^{-4}$, $u_b=5$, and $\alpha_b=1$. First, let us consider the case of $T_e/T_i=4$. In this case, the ion-sound wave damping should be higher than the previous case, and thus the decay process should, in principle, be able to proceed less efficiently than the case of $T_e/T_i=7$. Indeed, this appears to be partly true, as the top-right-hand panel shows. The initially constant level of the ion-sound mode is seen to quickly damp out over the entire q range, except near $q\sim0$ and $q\sim0.4$. However, it is important to note that the generation of the S mode by decay instability is still operative despite the relative low temperature ratio $T_e/T_i=4$, as the persistence of the bump on I_q^{+S} near $q\sim0.4$ shows.

Let us proceed further with the case of $T_e/T_i=10$, while all other parameters are held constant as before. The result corresponding to this value of temperature ratio is displayed in the middle panels of Fig. 8. The development of an ion-sound wave spectrum over time shows that the damping is less effective across the board, since the higher the ratio T_e/T_i, the lower the linear ion-sound damping rate. The similar trend can be observed in the case of an even higher value of $T_e/T_i=14$. Thus, we have confirmed a general trend that the higher the ratio T_e/T_i, the less efficient is the damping of the sound waves. However, we also find that even for a temperature ratio as low as $T_e/T_i=4$ (which is typical of the solar wind condition), the decay process is still effective.

We note that although at first sight the temperature ratio T_e/T_i should not affect the scattering off ions, the higher T_e/T_i nevertheless leads to a more efficient scattering. In short, the temperature ratio T_e/T_i influences both the decay and scattering processes. To understand this, we again go back to Eq. (13), and consider terms which depict scattering off ions. Note that both resonant velocities, $u=\pm3(q-q')/4$ and $u=\pm3(q+q')/4$, are substantially smaller than unity such that only the ions with velocities much smaller than their thermal velocity can participate in the scattering process. This can be seen by the fact that the quantity

$$u\,F_i=\frac{1}{\sqrt{\pi}}\left(\frac{m_i}{m_e}\frac{T_e}{T_i}\right)^{1/2}u\exp\left(-\frac{m_i}{m_e}\frac{T_e}{T_i}u^2\right),$$

which appears inside the scattering term, can be finite only if $(m_i/m_e)(T_e/T_i)\,u^2\ll1$. Therefore, the above quantity is not very sensitive to the change in T_e/T_i, since the resonant $u\ll1$ anyway. On the other hand, the induced scattering off the ions has an overall multiplicative factor of $2T_e/T_i$ in front, that is, the scattering coefficients in Eq. (13) have a factor $(2T_e/T_i)\,u\,F_i$. This means that the higher the ratio T_e/T_i, the larger the scattering coefficient.

An interesting and peculiar feature associated with Fig. 8 is the fact that as T_e/T_i increases, not only does the backscattered Langmuir wave intensity increase, but also the detailed shape of the wave spectrum near the end of the computation time becomes more structured. It is seen that both the primary and backscattered waves in the case of high T_e/T_i, such as 10 or 14, develop small-scale structures in q space associated with the wave number spectra, which cannot simply be attributed to the discreteness of the numerical q spectrum or numerical noise. Instead, this appears to a genuine result of actual physical processes. In order to investigate such a feature, we have again considered the reference case of $T_e/T_i=7$, but this time, we have computed the relevant equations for time interval twice as long as before, namely $0<\tau<2\times10^4$. The results are summarized in Fig. 9, where the distribution $F_e(u)$ and the L mode intensity $I_q^L(\tau)$ are plotted in the same format as before. Two features are prominent. The first is the clearly visible negative-u shoulder and the broad tail in the electron distribution, and the other is the development of small-scale structures in the wave intensity spectrum.

Our interpretation of these features is as follows: As we have noted, nonlinear wave-coupling processes beyond the quasilinear stage (the decay and the scattering off ions), can be simply stated as $L\rightarrow L'+S$ (and *vice versa*) and $L+i\rightarrow L'$. These processes lead to the enhanced peaks near $q\sim-0.2$ and $q\sim0$. Consider the backscattered mode, L' near $q\sim-0.2$. The L' wave interacts with the bulk electrons near $u=1/q\sim-1/0.2\approx5$, and gets partially absorbed by these electrons via Landau damping, while at the same time, also being scattered off ions again via the secondary process $L'+i\rightarrow L$, or undergo secondary decay $L'\rightarrow L+S$. The partial damping leads to the development of a negative-u plateau in the tail near $u\sim-5$. The secondary scattering and decay of an L' wave leads to the dumping of wave momenta back to the positive q domain which belongs to the primary Langmuir wave. However, each time the Langmuir waves are scattered off ions, their momenta is altered in accordance with the resonance condition, $u=3(q-q')/4\sim u_i$, where u_i is the normalized thermal speed of the ions, $u_i=(T_i/T_e)^{1/2}(m_e/m_i)^{1/2}$, or in the case of decay, the wave momentum difference is dictated by $q'=q\pm\eta$. In this way, the transfer of wave momentum from L' wave to L wave and

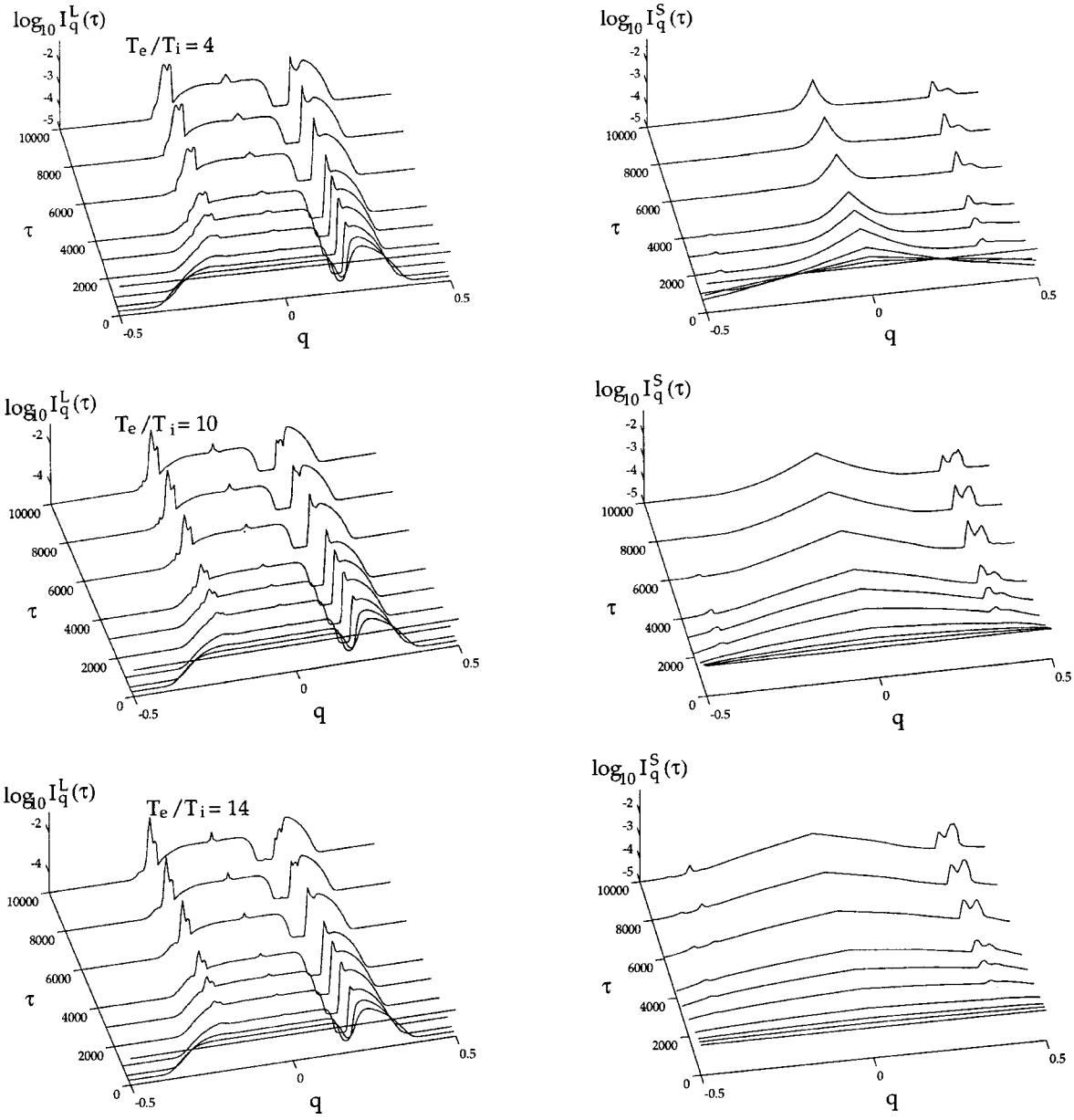

FIG. 8. Langmuir wave intensity $I_q^L(\tau)$, vs q and τ, for the case of $T_e/T_i=4$, 10, and 14. Other physical parameters are the same as in Fig. 2.

vice versa leads to the development of small-scale structure in the Langmuir-mode wave spectrum. This process repeats itself. The present finding that the Langmuir wave spectrum develops a fine structure in q, or equivalently, in k space, is in agreement with the heuristic analytical description of the backscattering process of Langmuir waves in terms of wave steepening and diffusion in k space.[72,73]

We could have pushed the numerical computation further in time to see whether the structures in the wave spectrum develops even further, but within the context of the present scheme which assumes that the ions are stationary, it is not very meaningful to consider extremely long-time behavior without allowing the ions to slowly respond. In fact, the normalized time $\tau=\omega_{pe}t=2\times10^4$ already corresponds to the ion plasma oscillation period $\omega_{pi}t\approx466$. This time period is mostly likely well into the ion quasilinear diffusion time. Another consideration which limits the applicability of the present approach to an extremely long-time behavior is the absence of the spontaneous fluctuations. In particular, the spontaneous scattering process is expected to broaden the wave spectrum such that the development of narrow striations in the wave spectrum is expected to be smoothed out somewhat.

As mentioned already, in the present formalism which ignores the spontaneously generated thermal fluctuation, the choice of initial wave level is somewhat arbitrary. Therefore, we sought to understand to what extent the choice of initial wave level affects the outcome of the numerical analysis. For this purpose, we decided to consider a case which is identical to the first case, namely, $n_b/n_0=2\times10^{-4}$, $T_e/T_i=7$, $u_b=5$, and $\alpha_b=1$, but $I_q^L(0)=I_q^S(0)=5\times10^{-4}$, instead of 2×10^{-4}. First, the evolution of the electron distribution function is shown in Fig. 10. As with the case shown in Fig. 1,

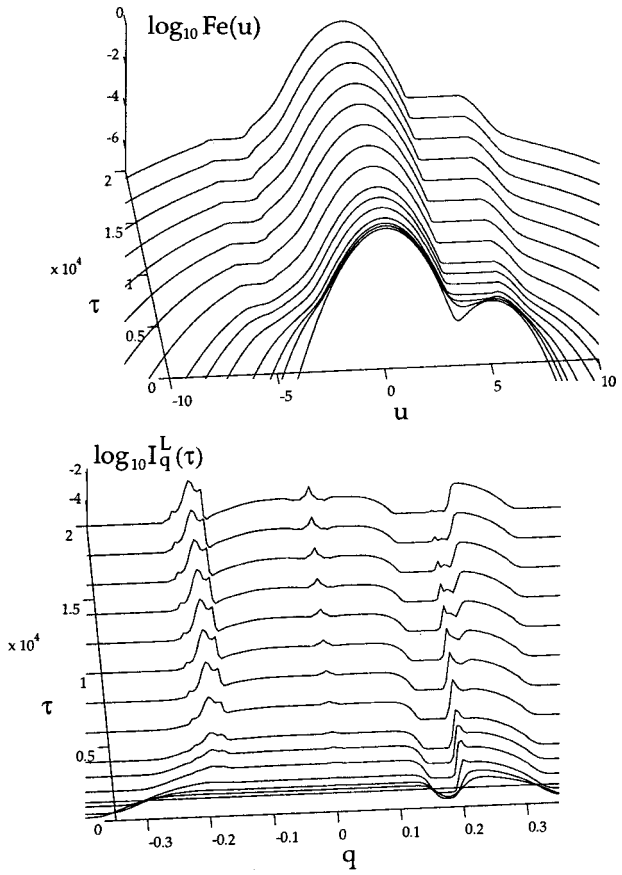

FIG. 9. A plot of electron distribution function, $F_e(u,\tau)$, vs u and τ, and Langmuir wave intensity $I_q^L(\tau)$ vs q and τ, for the same case as in Fig. 1, except that the final evolution time is twice as long as shown in Fig. 1, namely τ ranges from 0 to 2×10^4.

there is nothing particularly surprising as far as the development of electron beam distribution is concerned.

The corresponding wave spectra evolution is shown in Fig. 11. The left-hand panel shows logarithms of $I_q^L(\tau)$, while the right-hand panel shows $I_q^S(\tau)$. The format is the same as before. A noteworthy aspect of the present numerical result is that the ion-sound waves do not show any apparent development when compared with the case considered in Fig. 2. Unlike the previous case, no enhanced ion-sound waves appear in the spectrum, but instead the ion-sound waves damp out from the initial level over time. The ion-sound wave signature is often cited as the evidence for the decay process at work. From this, it might be concluded that the decay process is not effective in the present case of higher initial wave level. However, as we shall see, this is not the case. The decay process is still quite operative as far as the generation of backscattered and long-wavelength Langmuir modes are concerned. It is just that the product ion-sound wave intensity is not significant in this case.

The primary Langmuir wave spectrum follows the familiar pattern of initial exponential growth over an initially unstable domain around $q\sim0.2$, and exponential damping over the absorption region. The major difference is in the spectral characteristics associated with the Langmuir waves which results from the nonlinear processes, as shown in Fig. 11, in which $I_q^L(\tau)$ is plotted versus q and τ. Instead of the prominent peak near $q\sim-0.2$ and a smaller peak near $q=0$, as was seen in Fig. 2, we now have a higher peak near $q=0$, and a much lower peak near $q=-0.2$.

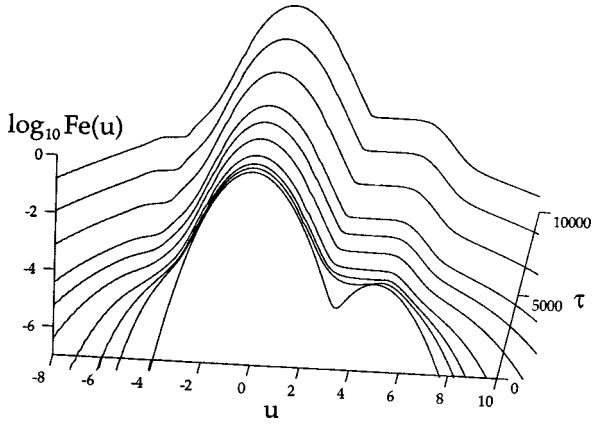

FIG. 10. A plot of electron distribution function, $F_e(u,\tau)$, vs u and τ, for the case of an initial wave level of $I_q^L(0)=I_q^S(0)=5\times10^{-4}$. Other parameters are the same as in Fig. 1, namely, $n_b/n_0=2\times10^{-4}$, $u_b=5$, and $T_e/T_i=7$.

In order to comprehend the result shown in Fig. 11, we have proceeded with the same steps taken previously. First, we turned off the induced-scattering effect, and only retained the three-wave decay terms. We have next solved the wave kinetic equation with the three-wave decay term turned off. The results of the two competing approximation schemes are shown in Fig. 12. These results can be compared with Figs. 5 and 6. As with Fig. 5, it can be seen that the decay instability leads to a weak growth of a Langmuir wave spectrum in the vicinity of $q=0$ and $q=-0.2$, which confirms our earlier statement that despite the apparent absence of enhanced ion-sound wave peaks, the decay process is nevertheless operative.

Note, the induced-scattering (off ions) also generates the modes in the similar spectral range over which the decay process is operative. This is, again, in agreement with the earlier case of lower initial wave intensity. Thus we conclude that despite the difference in the detailed spectral features, the relative roles of decay process versus induced-scattering process remains more or less the same as before, in that both processes lead to the generation of backscattered and long-wavelength Langmuir modes, and that the induced scattering is generally more effective. However, unlike the case shown in Fig. 6, the long-wavelength mode ($q\sim0$) possesses a much higher level of intensity when compared with the L wave near $q=-0.2$. This difference cannot be accounted for on the basis of any simple arguments.

To summarize the present findings, first, it can be surmised that by and large, the decay process, although weaker, does indeed contribute to the nonlinear wave-coupling process in a significant manner, but the induced-scattering off ions is the more efficient of the two. Second, the detailed numerical results of the two cases with different initial wave intensity are very different from each other in that the relative levels of backscattered versus long-wavelength Langmuir modes are reversed in the two cases. At the present time, we are not able to offer a simple explanation for such a discrepancy, but can only conclude that the nonlinear devel-

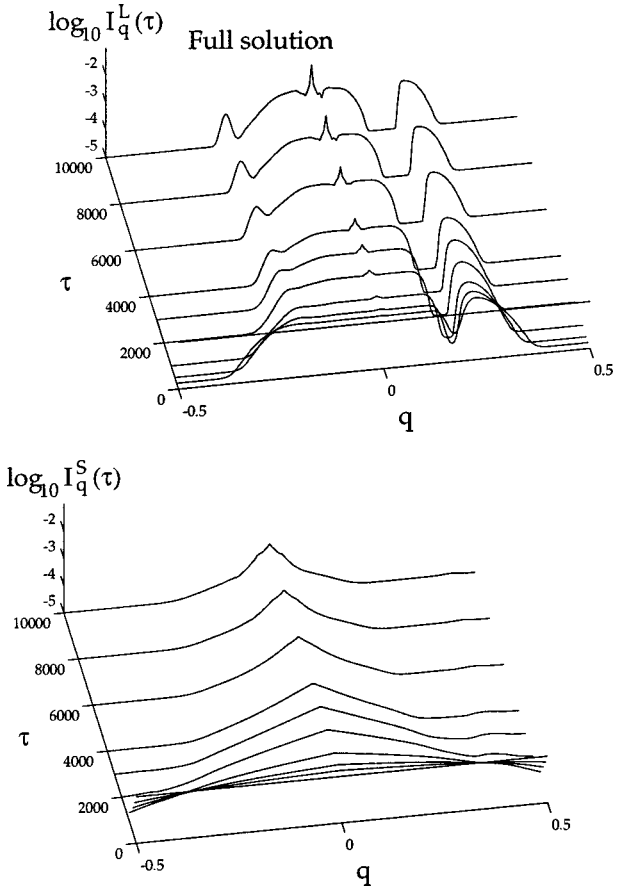

FIG. 11. A plot of Langmuir wave intensity, $I_q^L(\tau)$, and ion-sound wave intensity, $I_q^S(\tau)$, vs q and τ, corresponding to the case considered in Fig. 10. This solution corresponds to the solution of the complete wave kinetic equation including all the terms.

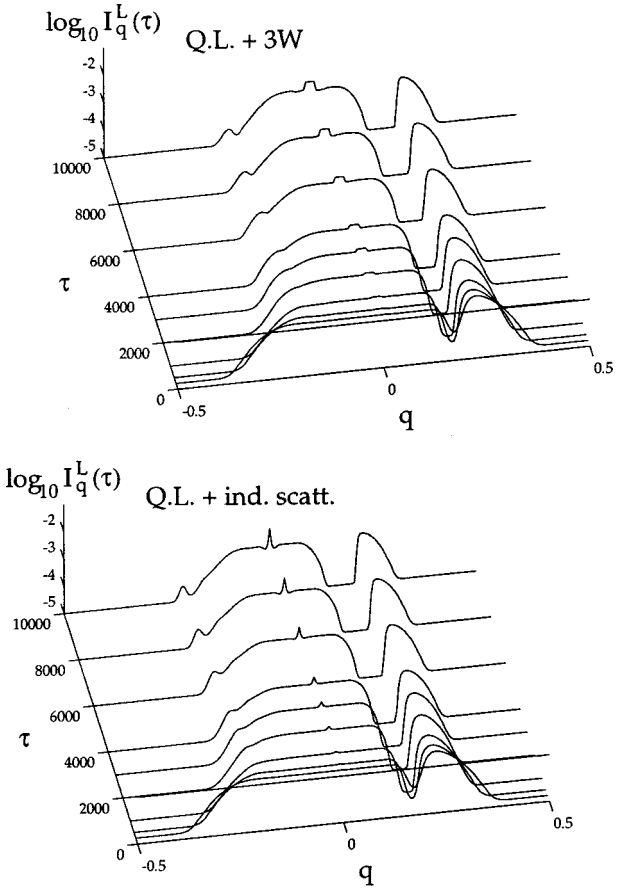

FIG. 12. A comparison of Langmuir wave intensities computed on the basis of a quasilinear plus three-wave approximation scheme vs the approximation in which only quasilinear plus induced scattering terms are kept.

opment of the instability is indeed very sensitive to the choice of initial wave level. This calls for a more systematic study in which various parameters, including the initial wave level and the beam speed, u_b, which we have not varied, and the temperature ratio between the background electrons and the beam electrons, which we have assumed to be equal, needs to be carried out. Moreover, an improved numerical computation is necessary in which the spontaneous thermal fluctuations and dynamic ions are included in the theory.

IV. CONCLUSIONS AND FUTURE DEVELOPMENTS

We have numerically solved the complete set of weak turbulence equations as found in the literature, which involves a quasilinear diffusion equation for the electrons and wave kinetic equations for Langmuir and ion-sound waves. The wave kinetic equations describe the induced emission, three-wave decay, and nonlinear induced scattering processes.

We find that the induced scattering of beam-excited Langmuir waves off the ions is an important nonlinear mechanism beyond the quasilinear stage,[36–38] but we also find that the three-wave decay process, although somewhat weaker, is quite significant such that it cannot be ignored at the outset. The induced scattering off ions is shown to generate Langmuir waves propagating in the opposite direction with respect to the primary Langmuir waves with comparable wavelength ($k_L' \sim -k_L$, where k_L denotes the wave number associated with the beam-excited primary Langmuir wave, and k_L' signifies the backscattered component), as well as a long-wavelength ($k \sim 0$) Langmuir wave component. The decay process is shown to operate in the similar spectral range as does the scattering of Langmuir waves by ions. It is also found that the generation of ion-sound waves, which is often cited as an indication of the decay process, is not necessarily always evident. Therefore, the present case studies have established the fact that the apparent absence of product ion-sound waves is not necessarily the indication that the decay process is ineffective.

It is found that the damping of the ion-sound waves becomes weaker as the ratio of electron to ion temperature, T_e/T_i, increases. Higher T_e/T_i should promote the activity of the three-wave decay process.[68] However, in general, we do not expect to find a circumstance, regardless of the value of T_e/T_i, where the decay process actually dominates over the scattering off ions, since the scattering off ions also becomes more efficient as T_e/T_i increases.

Finally, it is found that the initial level of wave intensity greatly affects the later outcome of the nonlinear spectrum of the waves. In particular, we find that the higher level of initial wave intensity leads to the prominent growth of long-wavelength Langmuir modes, while the backscattered com-

ponent is seen to be greatly diminished. Here, both the long-wavelength ($k \sim 0$) and backscattered ($k_L' \sim -k_L$) Langmuir waves are found to be produced as a result of combined induced-scattering off ions and the decay process. Therefore, the predominance of the long-wavelength Langmuir mode over the backscattered component seems to depend on the initial condition.

The limitations of the present study are first that the effects of spontaneously generated fluctuations are ignored. These fluctuations are generated by single-particle dynamics, which the Vlasov theory cannot account for. The importance of the spontaneous fluctuations is that they determine the initial wave level automatically so that one does not have to artificially model the initial wave level as we do in the present analysis. Moreover, the spontaneous scattering is expected to broaden the Langmuir wave spectrum. As a result, the detail spectral shape of the Langmuir turbulence spectrum is expected to be modified once the spontaneous fluctuation is incorporated in the theory.

The second shortcoming of the present approach is that the ions are considered as stationary. In order to discuss the long-time behavior in a rigorous manner, one has to take the ion dynamics into account. To consider the ion dynamics, one has to solve the ion quasilinear diffusion equation together with the electron equation. From the viewpoint of numerical analysis this is not so trivial since the ion thermal speed is much less than the electron thermal spread.

Finally, the present discussion is limited to the conventional treatment of beam–plasma instability in that the harmonic Langmuir waves (or the nonlinear eigenmode of a turbulent plasma discussed in Ref. 67) are not considered here. These and other aspects of nonlinear beam–plasma interaction physics, such as electromagnetic effects, need to be taken into consideration in the future.

ACKNOWLEDGMENTS

L.F.Z. and R.G. are thankful for the hospitality of the University of Maryland during their visit in the winter of 2001.

This research was supported by National Science Foundation Grant No. ATM 9905508 and the Department of Energy Grant DE-FG02-00ER54584 to the University of Maryland. L.F.Z. and R.G. acknowledge partial support by the Brazilian agencies Conselho Nacional de Desenvolvimento Científico e Tecnológico (CNPq) and Fundação de Amparo à Pesquisa do Estado do Rio Grande do Sul (FAPERGS).

[1] A. A. Vedenov, E. P. Velikhov, and R. Z. Sagdeev, Nucl. Fusion Suppl. **2**, 465 (1962).
[2] W. E. Drummond and D. Pines, Nucl. Fusion Suppl. **3**, 1049 (1962).
[3] A. Rogister and C. Oberman, J. Plasma Phys. **2**, 33 (1968).
[4] P. Nunez and S. Rand, Phys. Fluids **12**, 1666 (1969).
[5] G. Vahala and D. Montgomery, J. Plasma Phys. **4**, 677 (1970).
[6] T. Burns and G. Knorr, Phys. Fluids **15**, 610 (1972).
[7] K. Appert, T. M. Tran, and J. Vaclavik, Phys. Rev. Lett. **37**, 502 (1976).
[8] D. D. Ryutov and R. Z. Sagdeev, Sov. Phys. JETP **31**, 396 (1970).
[9] V. V. Zaitsev, N. A. Mityakov, and V. O. Rappoport, Sol. Phys. **24**, 444 (1972).
[10] R. J.-M. Grognard, Aust. J. Phys. **28**, 731 (1975).
[11] T. Takakura and H. Shibahashi, Sol. Phys. **46**, 323 (1976).
[12] G. R. Magelsson and D. F. Smith, Sol. Phys. **55**, 211 (1977).
[13] A. M. Vasquez and D. O. Gomez, Astrophys. J. **484**, 463 (1997).
[14] V. N. Mel'nik and E. P. Kontar, J. Plasma Phys. **60**, 49 (1998).
[15] V. N. Mel'nik, V. Lapshin, and E. Kontar, Sol. Phys. **181**, 353 (1999).
[16] D. F. Escande and G. V. de Genouillac, Astron. Astrophys. **68**, 405 (1978).
[17] D. F. Escande, Phys. Rev. Lett. **35**, 995 (1975); Phys. Fluids **22**, 321 (1979).
[18] B. B. Kadomtsev and V. I. Petviashvili, Sov. Phys. JETP **16**, 1578 (1963).
[19] L. M. Kovrizhnykh, Sov. Phys. JETP **21**, 744 (1965).
[20] B. B. Kadomtsev, *Plasma Turbulence* (Academic, New York, 1965).
[21] V. N. Tsytovich, Sov. Phys. Usp. **9**, 805 (1967).
[22] A. Rogister and C. Oberman, J. Plasma Phys. **3**, 119 (1969).
[23] R. Z. Sagdeev and A. A. Galeev, *Nonlinear Plasma Theory* (Benjamin, New York, 1969).
[24] V. N. Tsytovich, *Nonlinear Effects in a Plasma* (Plenum, New York, 1970).
[25] R. C. Davidson, *Methods in Nonlinear Plasma Theory* (Academic, New York, 1972).
[26] A. I. Akhiezer, I. A. Akhiezer, R. V. Polovin, A. G. Sitenko, and K. N. Stepanov, *Plasma Electrodynamics. Vol. 2. Nonlinear Theory and Fluctuations* (Pergamon, New York, 1975).
[27] V. N. Tsytovich, *An Introduction to the Theory of Plasma Turbulence* (Pergamon, New York, 1977).
[28] A. G. Sitenko, *Fluctuations and Nonlinear Wave Interactions in Plasmas* (Pergamon, New York, 1982).
[29] D. B. Melrose, *Plasma Astrophysics* (Gordon and Breach, New York, 1980).
[30] V. N. Tsytovich, *Lectures on Nonlinear Plasma Kinetics* (Springer-Verlag, New York, 1995).
[31] A. G. Sitenko and V. Malnev, *Plasma Physics Theory* (Chapman and Hall, New York, 1995).
[32] R. E. Aamodt and W. E. Drummond, Phys. Fluids **7**, 1816 (1964).
[33] M. E. Caponi and R. C. Davidson, Phys. Fluids **14**, 1463 (1971).
[34] P. A. Robinson, A. J. Willes, and I. H. Cairns, Astrophys. J. **408**, 720 (1993).
[35] S. D. Edney and P. A. Robinson, Phys. Plasmas **8**, 428 (2001).
[36] R. J.-M. Grognard, Solar Phys. **81**, 173 (1980); in *Solar Radiophysics*, edited by D. J. McLean and N. R. Labrum (Cambridge University Press, Cambridge, 1985), p. 253.
[37] C. T. Dum and R. N. Sudan, Phys. Fluids **14**, 414 (1971).
[38] L. Muschietti and C. T. Dum, Phys. Fluids B **3**, 1968 (1991).
[39] J. M. Dawson and R. Shanny, Phys. Fluids **11**, 1506 (1968).
[40] T. P. Armstrong and D. Montgomery, Phys. Fluids **12**, 2094 (1969).
[41] C. B. Wharton, J. H. Malmberg, and T. M. O'Neil, Phys. Fluids **11**, 1761 (1968).
[42] K. W. Gentle and C. W. Roberson, Phys. Fluids **14**, 2780 (1971).
[43] K. Mizuno and S. Tanaka, Phys. Rev. Lett. **29**, 45 (1972).
[44] K. W. Gentle and J. Lohr, Phys. Rev. Lett. **30**, 75 (1973).
[45] M. Seidl, W. Carr, D. Boyd, and R. Jones, Phys. Fluids **19**, 78 (1976).
[46] R. L. Morse and C. W. Nielson, Phys. Fluids **12**, 2418 (1969).
[47] G. Joyce, G. Knorr, and T. Burns, Phys. Fluids **14**, 797 (1971).
[48] A. J. Klimas, J. Geophys. Res. **88**, 9081 (1983).
[49] I. H. Cairns and K.-I. Nishikawa, J. Geophys. Res. **94**, 79 (1989).
[50] A. J. Klimas, J. Geophys. Res. **95**, 14905 (1990).
[51] C. T. Dum, J. Geophys. Res. **95**, 8095 (1990); **95**, 8111 (1990); **95**, 8123 (1990).
[52] K.-I. Nishikawa and I. H. Cairns, J. Geophys. Res. **96**, 19 343 (1991).
[53] C. T. Dum and K.-I. Nishikawa, Phys. Plasmas **1**, 1821 (1994).
[54] L. Yin, M. Ashour-Abdalla, M. El-Alaoui, J. M. Bosqued, and J. L. Bougeret, J. Geophys. Res. **103**, 29 619 (1998).
[55] D. Schriver, M. Ashour-Abdalla, V. Sotnikov, P. Hellinger, V. Fiala, R. Bingham, and A. Mangeney, J. Geophys. Res. **105**, 12 919 (2000).
[56] S. M. Levitskii and I. P. Shashurin, Sov. Phys. JETP **25**, 227 (1967).
[57] J. R. Apel, Phys. Rev. Lett. **19**, 744 (1967); Phys. Fluids **12**, 640 (1969).
[58] C. Roberson, K. W. Gentle, and P. Nielson, Phys. Rev. Lett. **26**, 226 (1971).
[59] G. Dimonte and J. H. Malmberg, Phys. Rev. Lett. **38**, 401 (1977); Phys. Fluids **21**, 1188 (1978).
[60] S. I. Tsunoda, F. Doveil, and J. H. Malmberg, Phys. Fluids B **3**, 2747 (1991).
[61] J. C. Adams, G. Laval, and D. Pesme, Phys. Rev. Lett. **43**, 1671 (1979).
[62] G. Laval and D. Pesme, Phys. Fluids **26**, 52 (1983); **26**, 66 (1983).
[63] G. Laval and D. Pesme, Phys. Rev. Lett. **53**, 270 (1984).

[64]K. Thielhaber, G. Laval, and D. Pesme, Phys. Fluids **30**, 3129 (1987).
[65]J. R. Cary, I. Doxas, D. F. Escande, and A. D. Verga, Phys. Fluids B **4**, 2062 (1992).
[66]Y.-M. Liang and P. H. Diamond, Phys. Fluids B **5**, 4333 (1993).
[67]P. H. Yoon, Phys. Plasmas **7**, 4858 (2000).
[68]I. H. Cairns, Phys. Plasmas **7**, 4901 (2000).
[69]There is a sign error in Eq. (18) of Ref. 67, where the overall sign associated with the various decay processes should be $+$.
[70]We detected a typographical error in Eq. (15) of Ref. 67, where the factor $(1+3T_i/T_e)^{1/2}$ is missing, and also in Eq. (23) where the ion distribution F_i is mistakenly written as F_e.
[71]W. H. Press, B. P. Flannery, S. A. Teukolsky, and W. T. Vetterling, *Numerical Recipes—The Art of Scientific Computing* (Cambridge University Press, Cambridge, 1989).
[72]Ya. B. Zeldovich, Usp. Fiz. Nauk **115**, 161 (1975).
[73]A. A. Galeev and R. Z. Sagdeev, in *Handbook of Plasma Physics*, Vol. 1, edited by A. A. Galeev and R. N. Sudan (North-Holland, New York, 1983), pp. 720–722.